

Synthesis of Silver Nanoparticles using Pulse Electrolysis in 1-n-butyl-3-methylimidazolium Chloride Ionic Liquid

Jeonggeun Jang¹, Jihee Kim¹, Churl Kyoung Lee^{2*}, and Kyungjung Kwon^{3*}

¹Samsung Electronics, 1 Samsung-ro, Yongin-si, Gyeonggi-do 17113, Korea

²School of Advanced Materials Science and Engineering, Kumoh National Institute of Technology, 1 Daehak-ro, Gumi, Gyeongbuk 39177, Korea

³Department of Energy & Mineral Resources Engineering, Sejong University, Seoul 05006, Korea

ABSTRACT

Ionic liquids are considered as a promising, alternative solvent for the electrochemical synthesis of metals because of their high thermal and chemical stability, relatively high ionic conductivity, and wide electrochemical window. In particular, their wide electrochemical window enables the electrodeposition of metals without any side reaction of electrolytes such as hydrogen evolution. The electrodeposition of silver is conducted in 1-n-butyl-3-methylimidazolium chloride ([C4mim]Cl) ionic liquid system with a silver source of AgCl. This study is the first attempt to electrodeposit silver nanoparticles without using co-solvents other than [C4mim]Cl. Pulse electrolysis is employed for the synthesis of silver nanoparticles by varying applied potentials from -3.0 V to -4.5 V (vs. Pt-quasi reference electrode) and pulse duration from 0.1 s to 0.7 s. Accordingly, the silver nanoparticles whose size ranges from 15 nm to ~100 nm are obtained. The successful preparation of silver nanoparticles is demonstrated regardless of the kinds of substrate including aluminum, stainless steel, and carbon paper in the pulse electrolysis. Finally, the antimicrobial property of electrodeposited silver nanoparticles is confirmed by an antimicrobial test using *Staphylococcus aureus*.

Keywords : Silver, Nanoparticle, Ionic Liquid, Pulse Electrolysis, 1-n-butyl-3-methylimidazolium Chloride

Received : 7 July 2022, Accepted : 10 August 2022

1. Introduction

Nanoparticles commonly signify clusters of atoms with the size range of 1~100 nm. Studies on metal nanoparticles have been conducted briskly in various applications because nanoparticles possess unique physical and chemical properties as against bulk metals. In particular, the usage of precious metals including platinum, palladium, gold, and silver could be minimized in the configuration of nanoparticles, which is beneficial to the application of precious metal nanoparticles to catalysts and sensors [1,2]. Among precious metals, silver nanoparticles possess antimicrobial, optical, and catalytic properties, which are dependent on their size distribution, structure, and

shape [3-9]. It is known that silver nanoparticles are effective on the growth inhibition of microorganism and antibacterial products containing silver nanoparticles are sold in large quantities worldwide [10,11]. Mechanisms behind the antimicrobial property of silver nanoparticles are usually provided in the following ways. Silver nanoparticles could impact directly on microorganism. Otherwise, anions dissolved from silver nanoparticles might inactivate microorganism [12-14].

Silver nanoparticles are typically produced via a liquid phase reduction method [3,4]. The liquid phase reduction method is effective for the synthesis of nanoparticles of regular-size distribution through controlling various synthesis conditions. Because colloid particles tend to aggregate mutually in a liquid phase due to their high surface energy, a surfactant such as polymer and thiol is commonly used as a protective material to stabilize colloid particles. This surfactant plays an important role in controlling the

*E-mail address: ckleee@kumoh.ac.kr, kfromberk@gmail.com

DOI: <https://doi.org/10.33961/jecst.2022.00570>

This is an open-access article distributed under the terms of the Creative Commons Attribution Non-Commercial License (<http://creativecommons.org/licenses/by-nc/4.0>) which permits unrestricted non-commercial use, distribution, and reproduction in any medium, provided the original work is properly cited.

size and shape of silver nanoparticles and their morphology modification is enabled in the process of vaporizing a liquid solvent [15-18].

Ionic liquids have received considerable attention as an alternative solvent for the electrochemical synthesis of metals because of their high thermal and chemical stability, relatively high ionic conductivity, and wide electrochemical window [19-23]. In addition, the ionic liquids are known to be eco-friendly solvents because they are reusable and do not generate volatile organic compounds [24,25]. In ionic liquids composed of imidazolium-based cations and chloride, 1-n-butyl-3-methylimidazolium chloride ([C4mim]Cl) is of interest as a green solvent due to its ability to be infinitely recycled and its amenability to solvation at room temperature. This kind of ionic liquid was first utilized for the electrodeposition of silver by combining aluminum chloride in the form of mixed room temperature molten salts [26]. Silver nanoparticles were electrochemically prepared in a quaternary ionic liquid microemulsion system including [C4mim]Cl [27,28].

In this work, we report the electrodeposition of silver nanoparticles in a single [C4mim]Cl ionic liquid system with a silver source of AgCl. To our knowledge, this study is the first attempt to electrodeposit silver nanoparticles without using co-solvents other than [C4mim]Cl. The prepared silver nanoparticles are further tested for antimicrobial effects.

2. Experimental

A three-electrode cell was used for the synthesis of silver nanoparticles. Aluminum alloy 6061, stainless steel 304, or carbon paper were used as the substrate of working electrode. Platinum wires (diameter 0.2 mm) were used as reference and counter electrodes. All electrodes were cleaned prior to use in a sonicating bath containing a solution of H₂SO₄ and H₂O₂ (1:1 vol.%). AgCl (Junsei Chemical Co., Ltd) was used as a silver source and [C4mim]Cl was used as an electrolyte for the electrodeposition. Linear sweep voltammetry (LSV) was performed using a potentiostat (SP-240, Bio-Logic) at a scan rate of 20 mV/s over a potential range between 0 V and -1.5 V (vs. Pt-quasi reference electrode (QRE)). Potentiostatic electrolysis of silver was conducted at -1.4 V (vs. Pt-QRE) for 2 h. Pulse electrolysis was also conducted by controlling pulse duration and overpotential

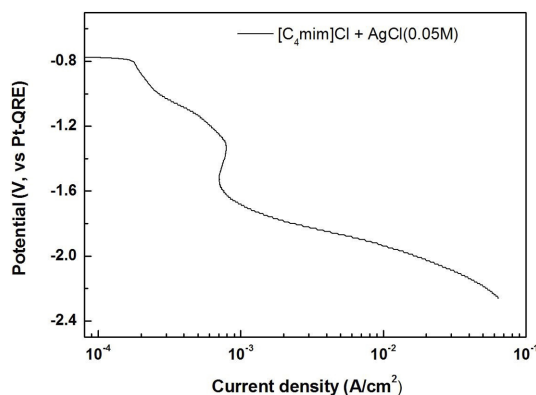


Fig. 1. LSV of Al 6061 electrode in the electrolyte of 0.05 M AgCl in [C4mim]Cl.

to synthesize silver nanoparticles. The morphology and chemical composition of electrodeposited silver were analyzed using a field emission scanning electron microscope (FE-SEM, JEOL, JSM-6701F).

3. Results and Discussion

3.1 Electrochemical reduction behavior of the electrolyte

The reduction behavior of silver was investigated using LSV at a scan rate of 20 mV/s. Fig. 1 shows the LSV of the electrolyte consisting of [C4mim]Cl and AgCl at Al 6061 working electrode. The reduction current starts to flow at -0.8 V and a limiting current behavior is observed from a potential of -1.4 V. As confirmed in the later parts of this manuscript, the reduction currents between -0.8 V and -1.4 V originate from the reduction of Ag⁺ to Ag. The reduction currents beyond the limiting current might be related to the Ag reduction and some side reactions of the ionic liquid.

Taking account the fact that the limiting current behavior appears at -1.4 V into account, the electrodeposition of silver was conducted under the potentiostatic condition at -1.4 V. Fig. 2 shows an FE-SEM image and the corresponding energy dispersive spectroscopy (EDS) analysis of silver electrodeposited on the Al 6061 electrode. The dendritic structure of silver was observed on the working electrode and the morphology of electrodeposited silver could vary by the degree of lattice mismatch between silver and substrate [29]. This dendritic morphology of silver is likely to result from the case where the lattice param-

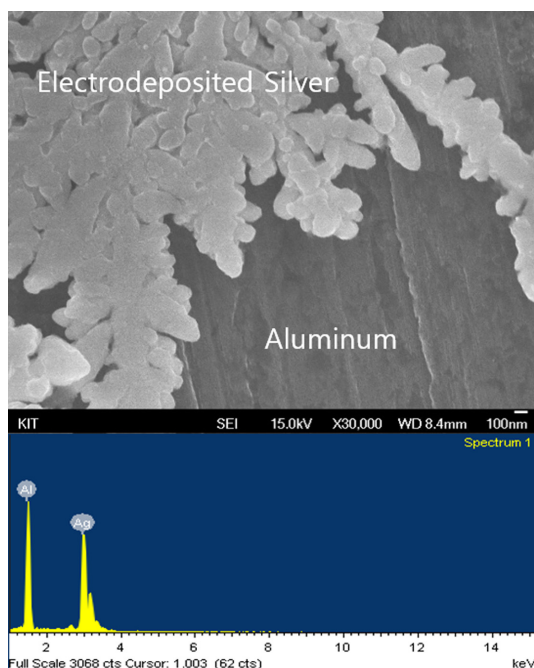


Fig. 2. FE-SEM/EDS of silver electrodeposited on the Al 6061 electrode at -1.4 V for 2 h.

eter of substrate is similar to the lattice parameter of silver that is formed by the aggregation of silver particles [30,31]. In addition, no impurity other than silver was detected in the EDS analysis.

3.2 Synthesis of silver nanoparticles using the pulse electrolysis

Fig. 3 is the FE-SEM image of the silver particles prepared by the pulse electrolysis at -3.0 V on the Al 6061 electrode. Even though the applied potential was lower than -1.4 V where the limiting current behavior appears, the decomposition of the ionic liquid was not apparent possibly due to a short span of applying the reduction potential ranging from 0.1 s to 0.7 s. Fig. 4 shows the size distribution of silver nanoparticles depending on the pulse duration from 0.1 s to 0.7 s in the pulse electrolysis at -3.0 V. The size of silver nanoparticles increases from 55 nm to ~100 nm with increasing the pulse duration. Under the potentiostatic pulse electrolysis at -3.0 V, the practically minimized pulse duration of 0.1 s was necessary to nucleate and grow 55 nm size of silver nanoparticles. The seven times increase of the pulse duration from 0.1 s to 0.7 s enlarged the silver nanoparticles twice from 55 nm to ~100 nm.

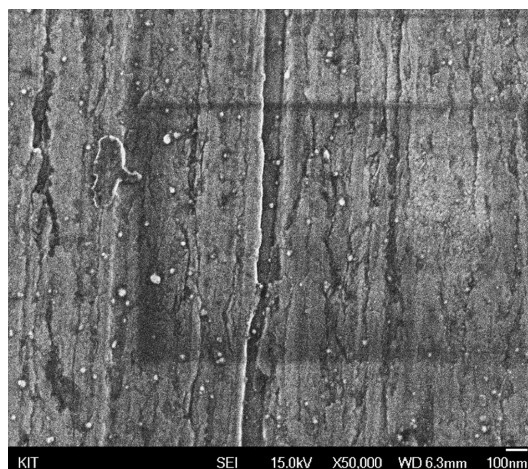


Fig. 3. FE-SEM image of silver nanoparticles synthesized by the pulse electrolysis at -3.0 V on the Al 6061 electrode in the electrolyte of 0.05 M AgCl in [C4mim]Cl.

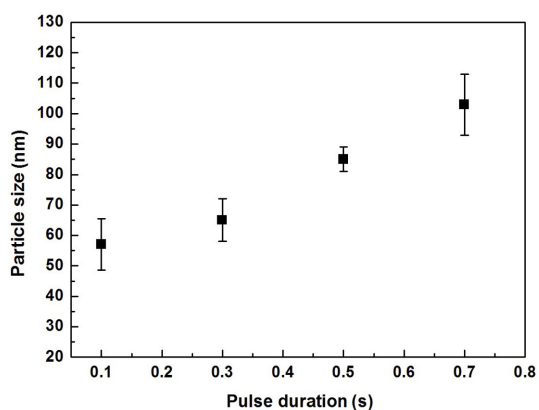


Fig. 4. Effect of the pulse duration on the particle size of electrodeposited silver in the pulse electrolysis.

To investigate the effect of the applied potential on the synthesis of silver nanoparticles, the potential was further extended to -4.5 V. As shown in Fig. 5, the negative increase in the applied potential decreased the size of silver nanoparticles from 55 nm to 15 nm. The decreasing particle size with the increasing overpotential for silver electrodeposition could be attributed to the imbalance between the enhancement of electron supply and the lack of Ag^+ supply due to the limiting current behavior at these potentials. In sum, the silver nanoparticles whose size ranges from 15 nm to ~100 nm can be obtained by the combination of the applied potential and the pulse

duration in the pulse electrolysis. However, a low applied potential less than -4.5 V would incur the decomposition of the ionic liquid although the short

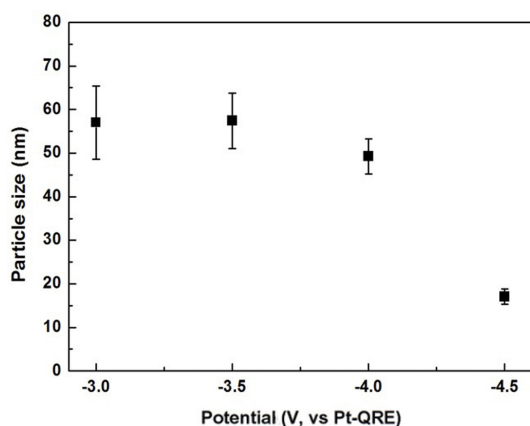


Fig. 5. Effect of the applied potential on the particle size of electrodeposited silver in the pulse electrolysis with 0.1 s of pulse duration.

span (0.1 s) of applying the reduction potential could minimize the reduction of the ionic liquid.

In order to examine the effect of substrate for the electrodeposition of silver nanoparticles, stainless steel 304 and carbon paper were additionally used as working electrodes. Fig. 6 shows the electrodeposited silver nanoparticles on both substrates under the same pulse electrolysis condition as Fig. 3. Although there is a slightly different size distribution of silver nanoparticles on stainless steel 304 and carbon paper from the case of Al 6061, the general feature of silver nanoparticles is similar regardless of the kinds of substrates. Thus, it could be concluded that the silver nanoparticles are successfully synthesized on any conductive substrates by the careful combination of the applied potential and the pulse duration in the pulse electrolysis.

3.3 Antimicrobial property of electrodeposited silver nanoparticles

An antimicrobial test was conducted by using a

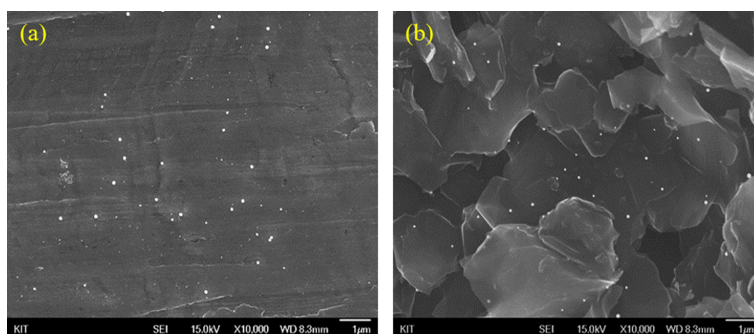


Fig. 6. FE-SEM image of electrodeposited silver nanoparticles on (a) stainless steel 304 and (b) carbon paper.

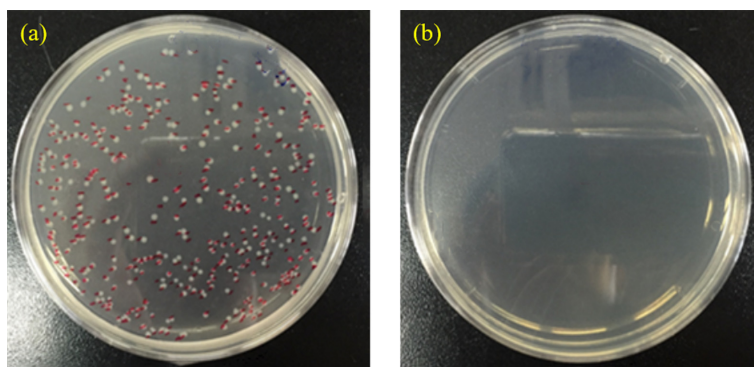


Fig. 7. Film attached method of *Staphylococcus aureus* on (a) untreated Al 6061 and (b) Al 6061 with electrodeposited silver nanoparticles.

film attached method with *Staphylococcus aureus* to confirm the antimicrobial property of electrodeposited silver nanoparticles. Fig. 7 presents a sharp contrast between the bare Al substrate and the electrodeposited silver nanoparticles on the Al substrate in terms of the number of bacteria colony. Whereas there was no visible colony on the Al substrate with silver nanoparticles, 348 colonies were detected on the bare Al substrate. Therefore, it is confirmed that the silver nanoparticles, which is prepared by the pulse electrolysis, have the antimicrobial activity.

4. Conclusions

The synthesis of silver nanoparticles was conducted by using the pulse electrolysis in a [C4mim]Cl ionic liquid system with AgCl. LSV demonstrated that the silver reduction starts to flow at -0.8 V vs. Pt-QRE and a limiting current behavior is observed from a potential of -1.4 V. The potentiostatic electrolysis at -1.4 V on the Al substrate produced the dendritic structure of silver without any impurity as confirmed by the EDS analysis. The pulse electrolysis was conducted by varying the applied potentials from -3.0 V to -4.5 V and the pulse duration from 0.1 s to 0.7 s. The silver nanoparticles whose size ranges from 15 nm to ~100 nm can be obtained by the combination of the applied potential and the pulse duration in the pulse electrolysis. Stainless steel 304 and carbon paper were additionally adopted as substrates for the electrodeposition of silver nanoparticles. It is concluded that the silver nanoparticles can be successfully synthesized on any conductive substrates by the pulse electrolysis. An antimicrobial test was conducted by using a film attached method with *Staphylococcus aureus* to confirm the antimicrobial property of electrodeposited silver nanoparticles.

Acknowledgements

This work was supported by Basic Science Research Program through the National Research Foundation of Korea (NRF) funded by the Ministry of Education (2020R1A6A1A03038540) and the Ministry of Science and ICT (2020R1F1A1053911).

References

- [1] K. Kwon, K. H. Lee, D. H. Um, S. Jin, H. S. Park, J. Cho, J. Hyun, H. C. Ham, and C. Pak, *J. Ind. Eng. Chem.*, **2021**, *97*, 280-286.
- [2] D. J. You, K. Kwon, S. H. Joo, J. H. Kim, J. M. Kim, C. Pak, and H. Chang, *Int. J. Hydrog. Energy*, **2012**, *37*(8), 6880-6885.
- [3] S. Irvani, H. Korbekandi, S. V. Mirmohammadi, and B. Zolfaghari, *Res. Pharm. Sci.*, **2014**, *9*(6), 385-406.
- [4] K. M. M. A. El-Nour, A. Eftaiha, A. Al-Warthan, and R. A. A. Ammar, *Arab. J. Chem.*, **2010**, *3*(3), 135-140.
- [5] M. Rai, A. Yadav, and A. Gade, *Biotechnol. Adv.*, **2009**, *27*(1), 76-83.
- [6] S. Gurunathan, K. Kalishwaralal, R. Vaidyanathan, D. Venkataraman, S. R. K. Pandian, J. Muniyandi, N. Hariharan, and S. H. Eom, *Colloid. Surf. B*, **2009**, *74*(1), 328-335.
- [7] K. Shameli, M. B. Ahmad, E. A. J. Al-Mulla, N. A. Ibrahim, P. Shabanzadeh, A. Rustaiyan, Y. Abdollahi, S. Bagheri, S. Abdolmohammadi, M. S. Usman, and M. Zidan, *Molecules*, **2012**, *17*(7), 8506-8517.
- [8] B. R. Cuenya, *Thin Solid Films*, **2010**, *518*(2), 3127-3150.
- [9] A. Singh, D. Jain, M. K. Upadhyay, N. Khandelwal, and H. Verma, *Dig. J. Nanomater. Biostructures*, **2010**, *5*(2), 483-489.
- [10] S. Saravanan, S. Nethala, S. Pattnaik, A. Tripathi, A. Moorthi, and N. Selvamurugan, *Int. J. Biol. Macromol.*, **2011**, *49*(2), 188-193.
- [11] R. Kaegi, B. Sinnet, S. Zuleeg, H. Hagendorfer, E. Mueller, R. Vonbank, M. Boller, and M. Burkhardt, *Environ. Pollut.*, **2010**, *158*(9), 2900-2905.
- [12] K. Chaloupka, Y. Malam, and A. M. Seifalian, *Trends Biotechnol.*, **2010**, *28*(11), 580-588.
- [13] Y. Yang, J. Wang, Z. Xiu, and P. J. J. Alvarez, *Environ. Toxicol. Chem.*, **2013**, *32*(7), 1488-1494.
- [14] I. Sondi and B. Salopek-Sondi, *J. Colloid Interface Sci.*, **2004**, *275*(1), 177-182.
- [15] D. Debnath, C. Kim, S. H. Kim, and K. E. Geckeler, *Macromol. Rapid Commun.*, **2010**, *31*(6), 549-553.
- [16] I. Pardinan-Blanco, C. E. Hoppe, M. A. Lopez-Quintela, and J. Rivas, *J. Non-Cryst. Solids*, **2007**, *353*(8-10), 826-828.
- [17] V. V. Makarov, A. J. Love, O. V. Sinitsyna, S. S. Makarova, I. V. Yaminsky, M. E. Taliansky, and N. O. Kalinina, *Acta Naturae*, **2014**, *6*(1), 35-44.
- [18] A. N. Shipway, E. Katz, and I. Willner, *ChemPhysChem*, **2000**, *1*(1), 18-52.
- [19] Y. Lu, K. Korf, Y. Kambe, Z. Tu, and L. A. Archer, *Angew. Chem. Int. Ed.*, **2014**, *53*(2), 488-492.
- [20] J.-O. Lee, G. Park, J. Park, Y. Cho, and C. K. Lee, *Int. J. Precis. Eng. Manuf.*, **2015**, *16*, 1229-1232.
- [21] Y. Jung, B. Dilasari, W.-S. Bae, H.-I. Kim, and K. Kwon, *RSC Adv.*, **2020**, *10*, 24115-24118.
- [22] B. Dilasari, Y. Jung, G. Kim, and K. Kwon, *ACS Sustain. Chem. Eng.*, **2016**, *4*(2), 491-496.
- [23] J. Park, C. K. Lee, K. Kwon, and H. Kim, *Int. J. Electrochem. Sci.*, **2013**, *8*, 4206-4214.
- [24] S. Zhang, N. Sun, X. He, X. Lu, and X. Zhang, *J. Phys.*

- Chem. Ref. Data*, **2006**, 35, 1475-1517.
- [25] J. Park, Y. Jung, P. Kusumah, J. Lee, K. Kwon, and C. K. Lee, *Int. J. Mol. Sci.*, **2014**, 15(9), 15320-15343.
- [26] F. Endres and W. Freyland, *J. Phys. Chem. B*, **1998**, 102(50), 10229-10233.
- [27] Y. Li, Q. Qiang, X. Zheng, and Z. Wang, *Electrochem. Commun.*, **2015**, 58, 41-45.
- [28] Y. Li, Z. Wang, and C. Zhao, *J. Electrochem. Soc.*, **2016**, 163(8), D442-D446.
- [29] J. Yu and X. Zhou, *Adv. Mater. Sci. Eng.*, **2013**, 2013, 519294.
- [30] C. L. Liang, K. Zhong, M. Liu, L. Jiang, S. K. Liu, D. D. Xing, H. Y. Li, Y. Na, W. X. Zhao, Y. X. Tong, and P. Liu, *Nano-Micro Lett.*, **2010**, 2, 6-10.
- [31] M. Miranda-Hernández, I. González, and N. Batina, *J. Phys. Chem. B*, **2001**, 105(19), 4214-4223.